Dissipation and dispersion control of a quadratic-reconstruction advection scheme

Alexandre CARABIAS Alain DERVIEUX

INRIA Sophia-Antipolis
Project TROPICS
Alain.Dervieux@inria.fr

European Workshop on High Order Nonlinear Numerical Methods for Evolutionary PDEs: Theory and Applications, Trento, Italy, april 11-15, 2011

Motivations (1)

Context of the present study

In Fluid Mechanics, most industrial computations are performed with second-order accurate schemes but do not enjoy second order numerical convergence (as for example measured by the Convergence Grid Index).

Reasons are singularities or more generally too many details (of various scales) to capture.

Consequences are waste (of theoretical accuracy) and less chances to evaluate error.

Motivations (2)

Some conditions for an fiable numerical convergence, possibly close to the theoretical one:

- *anisotropic mesh adaption,*

- *governed by an error analysis (from a well-specified goal)*

High-Accuracy Edge-Based scheme (Cf. T. Kozubskaya's talk) with TVD limiter. [Loseille-Alauzet-Dervieux,JCP-2010]

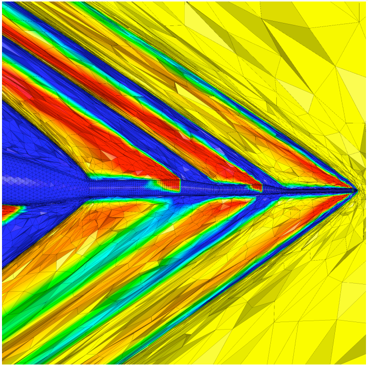

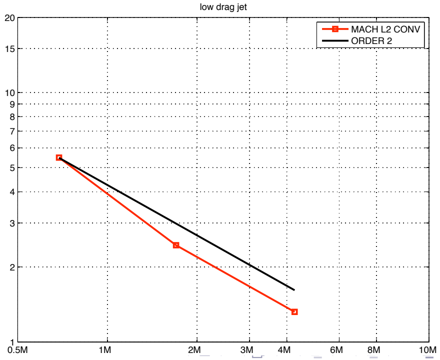

Motivations (3): advection, first example

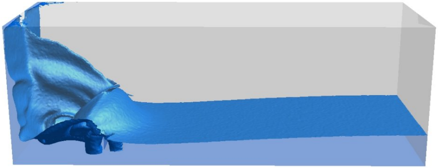

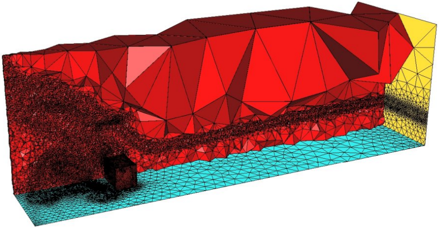

Level set adaptive tracking in an unstructured mesh

- High-Accuracy Edge-Based scheme (HAEB) with *no* limiter.

- Second order numerical convergence.

[Guegan-Allain-Dervieux-Alauzet,IJNME-2010]

Motivations (4): advection, second example

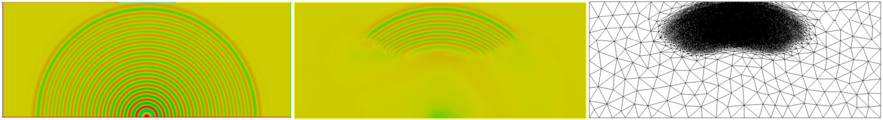

Acoustics wave adaptive capturing in an unstructured mesh

- HAEB with no limiter.
- Second order numerical convergence.

[Belme et al. to appear]

Towards a better advection scheme

The three previous examples were performed with HAEB scheme presented by T. Kozubskaya and enjoying:
- low dissipation (fifth-order accurate on cartesian meshes)
- *only* second-order accurate on unstructured meshes,

Requirements for a better scheme

Coarse mesh accuracy, low dissipation, small computing effort for a given mesh:

- Central-ENO (cf. C. Groth) reconstruction,

- Vertex centered approximation,

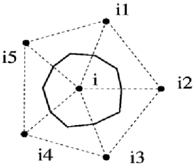

Plan of the talk

1. Baseline 2D quadratic scheme.
2. Analysis and improvement of a 1D context.
3. Extension to 2D.
4. Preliminary numerical experiments.

1. Baseline scheme (1)

Vertex, dual cell, 2-exact Central-ENO quadratic reconstruction

Given $\bar{u}_i$ on on each cell i of centroid G_i, find the $c_{i,\alpha}$, $|\alpha| \le k$ such that

$$\overline{P_{i,i}} = \overline{u_i} \qquad \sum_{j \in N(i)} (\overline{P_{i,j}} - \overline{u_j})^2 = Min$$

with

$$P_i(x) = \bar{u}_i + \sum_{|\alpha| \le k} c_{i,\alpha} [(X - G_i)^\alpha - \overline{(X - G_i)^\alpha}]$$

and where $\overline{P_{i,j}}$ stands for the mean of $P_i(x)$ on cell j.

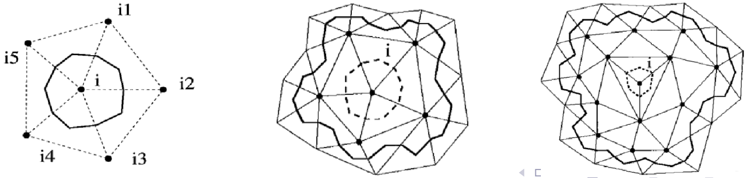

1. Baseline scheme (2)

2-exact flux integration

The integral on a cell interface $C_{ij} = C_i \cap C_j$ is split into the integrals on the two segments of C_{ij}.

On each segment $C_{ij}^{(1)}$ and $C_{ij}^{(2)}$ a numerical integration with two Gauss points (two Riemann solvers) is applied.

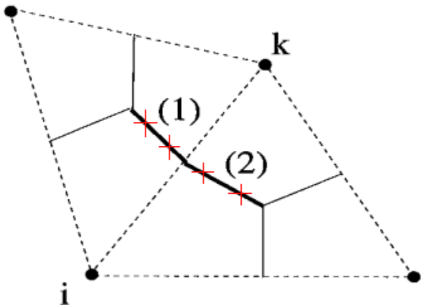

1. Baseline scheme (3)

Computational cost, fixed mesh

Computational cost is minimised by computing and storing reconstruction topology, coefficients and inverse matrix.

This needs be done each time mesh is changed.

In these conditions, the quadratic reconstruction scheme at each time step needs for each flux evaluation between two cells:

4 Riemann solutions,

where 1 is needed with the HAEB. We have check that the overall CPU ratio is more than 4.

Computational cost, changing mesh

In the case of a moving mesh the ratio between MUSCL and quadratic is more than 6.

These are 2D measures and should much amplify for 3D.

A test case: C.Tam's test for linear acoustics

[Ouvrard-Kozubskaya-Abalakin-Koobus-Dervieux, INRIA Rep. 2009]

- 12 Δx per bandwidth, three types of mesh.
- **black**: HAEB scheme,
- **Blue**: the present CENO2 scheme.

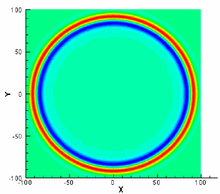

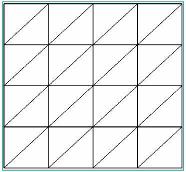

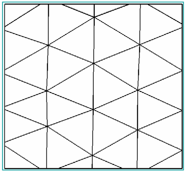

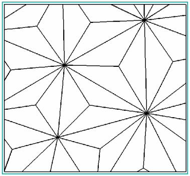

Mesh1	Mesh1	Mesh2	Mesh2	Mesh3	Mesh3
L^1	L^2	L^1	L^2	L^1	L^2
1.3045D-3	2.8561D-3	1.2786D-3	2.6318D-3	3.1097D-3	5.9216D-3
1.5189D-4	3.4010D-4	3.7384D-4	2.6318D-3	6.7626D-4	1.4598D-3

2. Analysis and improvement of a 1D context

Upwind Finite Volumes

$$\bar{u}_i = \frac{1}{\Delta x}\int_{C_i} u(x,t)dx \qquad C_i = [x_{i-1/2}, x_{i+1/2}].$$

$$\frac{\partial}{\partial t}\bar{u}_i + \frac{1}{\Delta x}\left[\Phi(u^+_{i+1/2}, u^-_{i+1/2}) - \Phi(u^+_{i-1/2}, u^-_{i-1/2})\right] = 0$$

$$\Phi_{upwind}(u^+_{i+1/2}, u^-_{i+1/2}) = c\frac{u^+_{i+1/2} + u^-_{i+1/2}}{2} - \delta|c|\frac{u^+_{i+1/2} - u^-_{i+1/2}}{2} \quad (*)$$

Polynomial reconstruction

$$u_i^{recons}(x) = P_i^{\bar{u}}(x - x_i)$$

P polynomial of degree k, such that for any u is a polynomial of degree k, we have

$$u_i^{recons} = u \quad \forall \ i,$$

then (*) holds exactly (P_k exactness).

Analysis and improvement of a 1D context (2)

For example, with a quadratic reconstruction and **uniform** mesh:

$$u_i^{recons}(x) = c_i + b_i(x - x_i) + a_i(x - x_i)^2$$

$$a_i = \frac{\bar{u}_{i+1} - 2\bar{u}_i + \bar{u}_{i-1}}{2\Delta x^2}$$

$$b_i = \frac{\bar{u}_{i+1} - \bar{u}_{i-1}}{2\Delta x}$$

$$c_i = \frac{-\bar{u}_{i+1} + 2\bar{u}_i - \bar{u}_{i-1}}{24} + \bar{u}_i$$

Analysis and improvement of a 1D context (3)

Spatial truncation analysis

$$\bar{u}_i = u_i + u_i^{(2)} \frac{\Delta x^2}{24} + u_i^{(4)} \frac{\Delta x^4}{1920} + O\left(\Delta x^6\right).$$

$$\int_{C_i} \frac{\partial u}{\partial x}\, dx - \frac{1}{\Delta x}\left[\Phi(u^+_{i+1/2}, u^-_{i+1/2}) - \Phi(u^+_{i-1/2}, u^-_{i-1/2})\right] =$$

$$-\frac{\delta |c|}{12}(\Delta x)^3 u^{(4)} + \frac{|c|}{30}(\Delta x)^4 u^{(5)} + O\left(\Delta x^6\right).$$

- Diffusion is the largest term of truncation error, with a large influence for coarse meshes.

- Dispersion vs diffusion balance contributes to the "Essentially Non Oscillating" effect which masters the possible oscillations provoked by singularities.

- This balance makes diffusion unnecessarily large for smooth solutions.

FD Analysis of P_k exact reconstructions

Passing to a 3-rd degree polynomial reconstruction:

- would add an $\Delta x^3 u^{(3)}$ term in the interpolations,

which will become, through the Riemann solver and the final divergence,
(1) a $\Delta x^4 u^{(5)}$ term and
(2) a $\Delta x^3 u^{(4)}$ one.
The first term in error contributes to a $\Delta x^4 u^{(5)}$ dispersion one.
The second one will *compensate* the diffusion of the quadratic scheme.

Putting $\delta = 0$ (no diffusive term) in the quadratic scheme is enough for getting rid of the $\Delta x^3 u^{(4)}$ term and reach 4-th order accuracy (with a probable lack of dissipation). The first term in error becomes a $\Delta x^4 u^{(5)}$ dispersion one just as for the extension to cubic.

Let us boost our quadratic scheme

What

- Reduce the diffusion model from a $(\Delta x)^3 u^{(4)}$ term to a $(\Delta x)^5 u^{(6)}$ term.
- Improve the dispersion vs diffusion balance by reducing the dispersion.

How

- The quadratic reconstruction is kept, with only contribution into the *centered* part of the Riemann solver.
- An approximate fourth-order derivative is obtained from the second derivative $u_h'' = 2a_i$ built by the quadratic reconstruction by divided differences

$$u_h^{(4)} = \frac{2}{\Delta x}(a_{i+1} - 2a_i + a_{i-1})$$

and introduced (with $(\Delta x/2)^4/4!$ factor) in the *diffusive* part of the Riemann solver.
- An approximate third-order derivative is obtained similarly

$$u_h^{(3)} = \frac{1}{\Delta x}(a_{i+1} - a_{i-1})$$

and introduced in the *centered* part of the Riemann solver.

Introducing 5-th order 6-th derivative diffusion

Reconstruction model:

$$u_{reconstr}(x+x_i) = \hat{u}_h + u_h' x + \frac{1}{2} u_h'' x^2 + \frac{1}{3!} u_h^{(3)} x^3 + \frac{1}{4!} u_h^{(4)} x^4$$

$\hat{u}_h + u_h' x + \frac{1}{2} u_h'' x^2$ is put in the *centered* part of Riemann solver,

$\frac{1}{3!} u_h^{(3)} x^3$ is put in the *centered* part of Riemann solver,

$\frac{1}{4!} u_h^{(4)} x^4$ is put in the *diffusive* part of Riemann solver.

A fifth-order linearised Runge-Kutta explicit time advancing is applied.

Properties of the 1D prototype

The above scheme is fifth-order accurate for uniform meshes.

Some numerical 1D experiments (1)

Advection of a sinus

Cartesian meshes starting from 4.

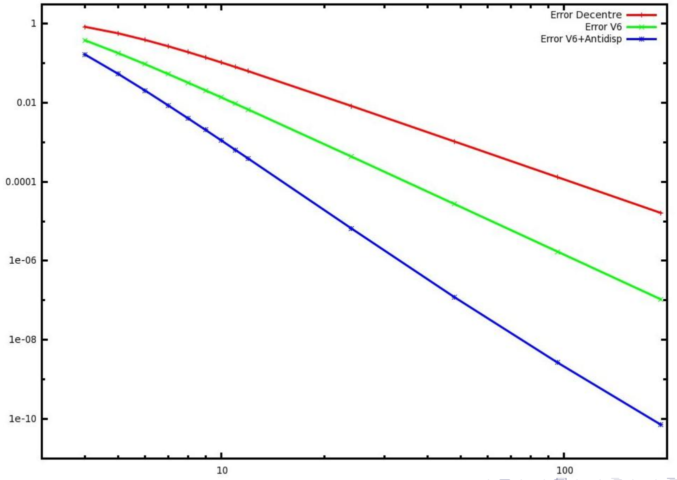

Some numerical 1D experiments (2)

Numerical convergence analysis

Mean values at cell centers: approximate (green) and exact (red)solutions for a travel of 100 wavelengths (CFL=.9) and 12 nodes per wavelength.

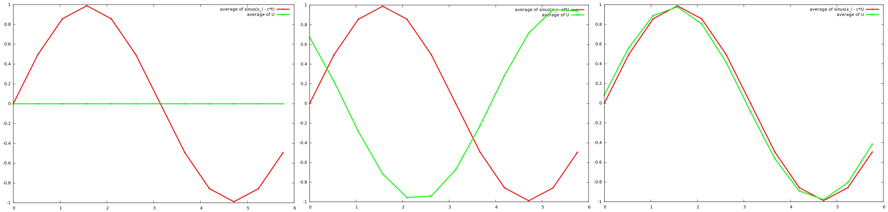

– Baseline scheme – Central+V6-diffusion – Central+V6+antidispersion

3. Extension to 2D

Main principle

- Our concern is to avoid a large increase the computational cost with respect to the baseline quadratic reconstruction scheme.

- We start from this baseline quadratic scheme.

- The two above corrections are applied on an edge-based mode.

- They are computed in the 1D direction of edge *ik* from interpolations of the approximate Hessians given by the quadratic reconstruction.

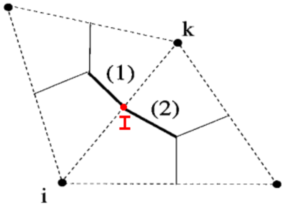

Extension to 2D (3)

Reconstruction model:

$$u_{reconstr}(\mathbf{x}_i + \delta\mathbf{x}) = \hat{u}_h + u_h' \cdot \delta\mathbf{x} + \frac{1}{2} u_h'' \cdot \delta\mathbf{x} \cdot \delta\mathbf{x} + \frac{1}{3!}\frac{\partial^3 u_h}{\partial s^3}(\delta s)^3 + \frac{1}{4!}\frac{\partial^4 u_h}{\partial s^4}(\delta s)^4$$

$\hat{u}_h + u_h' \cdot \delta\mathbf{x} + \frac{1}{2} u_h'' \cdot \delta\mathbf{x} \cdot \delta\mathbf{x}$ is computed on each of the *four Gauss integration points*

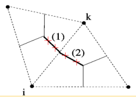

G_1, G_2, G_3, G_4 of the interface ∂C_{ij}: $\delta\mathbf{x} = \mathbf{x}_{G_k} - \mathbf{x}_i$ i=1,4 and put in the *centered* part of Riemann solver ,

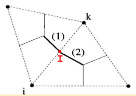

$\frac{1}{3!}\frac{\partial^3 u_h}{\partial s^3}(\delta s)^3$ is computed on *edge middle I* ($\delta s = ||ij||/2$) and put in the *centered* part of Riemann solver,

$\frac{1}{4!}\frac{\partial^4 u_h}{\partial s^4}(\delta s)^4$ is computed on *edge middle I* and put in the *diffusive* part of Riemann solver.

$\Rightarrow$ Less than extra 40 flops by edge.

4. Some preliminary numerical experiments

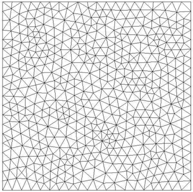

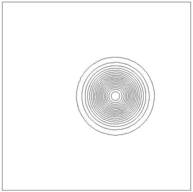

4.1.-Advection of a Gaussian

4.2.-Advection of the isovalue of a two-Gaussian camel hump.

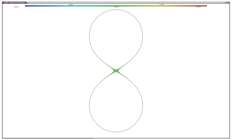

Numerical experiments

Convection of a Gaussian concentration, **structured** meshes.

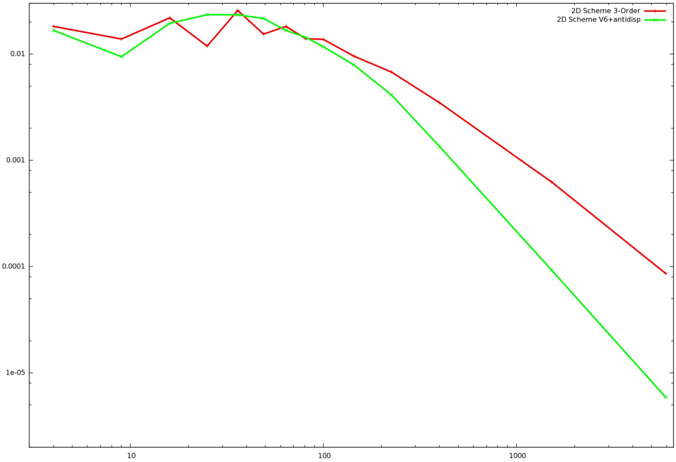

Numerical experiments

Convection of a Gaussian concentration, **unstructured** meshes

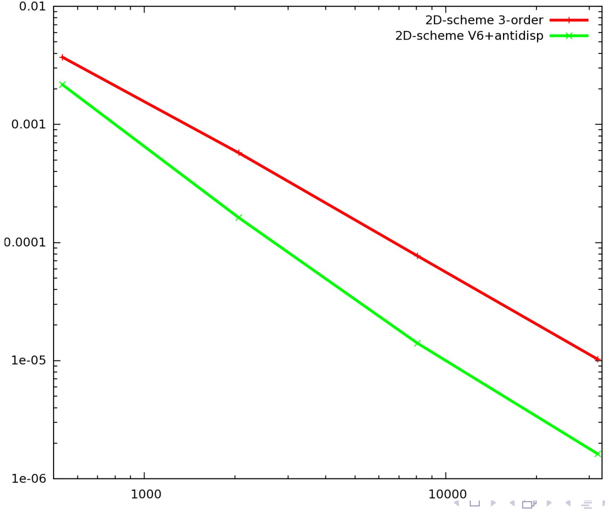

Numerical experiments

Convection of a sum of two Gaussian concentration, evolution of an isovalue.
Mesh 201 $\times$ 201. 50 points per wavelength. Initial condition.

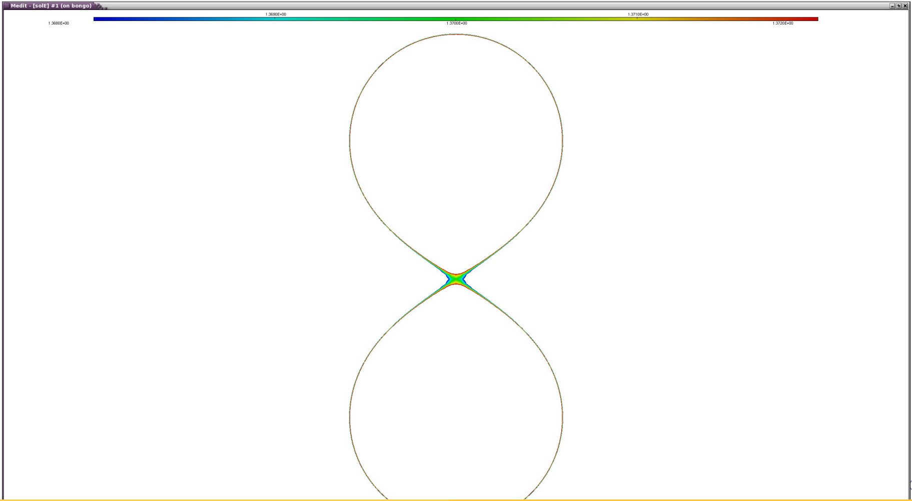

Numerical experiments

Convection of a sum of two Gaussian concentration, evolution of an isovalue. Mesh 201×201. 50 points per wavelength. Baseline scheme.

4. Numerical experiments (5)

Numerical experiments

Convection of a sum of two Gaussian concentration, evolution of an isovalue. Mesh 201×201. 50 points per wavelength. Scheme with new viscosity.

4. Numerical experiments (6)

Numerical experiments

Convection of a sum of two Gaussian concentration, evolution of an isovalue.
Mesh 201×201. 50 points per wavelength. New scheme.

Numerical experiments

Convection of a sum of two Gaussian concentration, evolution of an isovalue. Mesh 21×21. 5 points per wavelength. Initial condition.

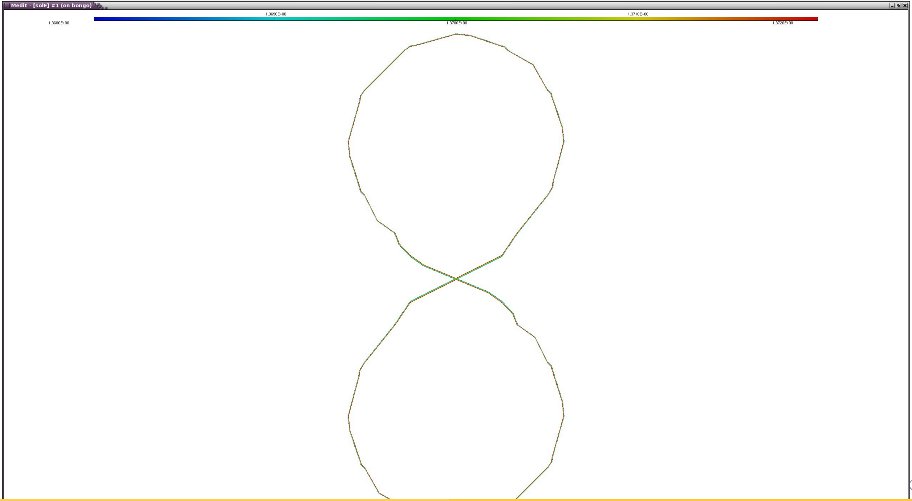

4. Numerical experiments (8)

Numerical experiments

Convection of a sum of two Gaussian concentration, evolution of an isovalue.
Mesh 201 $\times$ 201. 5 points per wavelength. Baseline scheme.

Numerical experiments

Convection of a sum of two Gaussian concentration, evolution of an isovalue.
Mesh 21×21. 5 points per wavelength. Scheme with new viscosity.

Numerical experiments

Convection of a sum of two Gaussian concentration, evolution of an isovalue.
Mesh 21×21. 5 points per wavelength. New scheme.

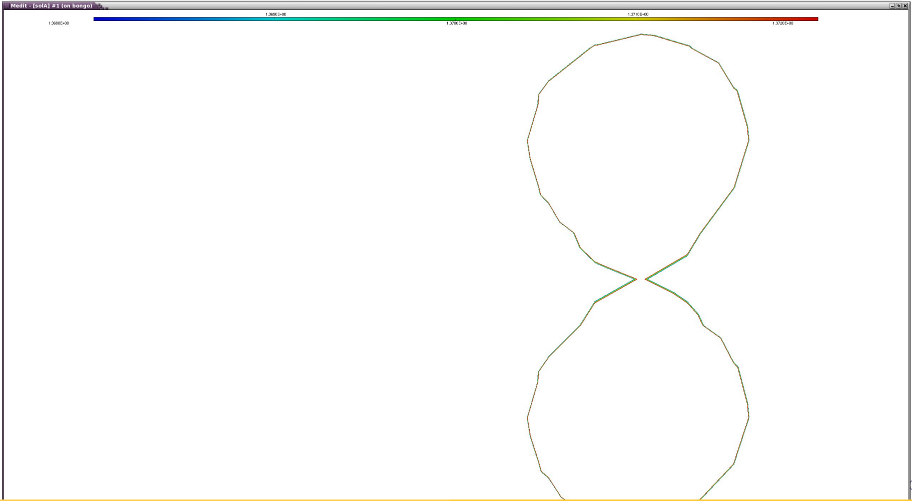

5. Extension to the Euler's equations (1)

Euler equations

$$\frac{\partial W}{\partial t} + \nabla . F(W) = 0,$$

with $W = (\rho, \rho u, \rho v, \rho w, \rho E)^t$ is the conservative variable vector and F is the convection operator $F(W) = \big(F_1(W), F_2(W), F_3(W)\big)$:

Convection operator

$$F_1(W) = \begin{pmatrix} \rho u \\ \rho u^2 + p \\ \rho uv \\ \rho uw \\ (\rho E + p)u \end{pmatrix}, F_2(W) = \begin{pmatrix} \rho v \\ \rho uv \\ \rho v^2 + p \\ \rho vw \\ (\rho E + p)v \end{pmatrix}, F_3(W) = \begin{pmatrix} \rho w \\ \rho uw \\ \rho vw \\ \rho w^2 + p \\ (\rho E + p)w \end{pmatrix}.$$

5. Extension to the Euler's equations (2)

Finite Volume applied to Euler's Equation

$$|C_i|\frac{dW_i}{dt} + \int_{\partial C_i} F(W_i).\mathbf{n}_i d\gamma - \int_{\Gamma_h \cap \partial C_i} \hat{F}(W_i).n_{\Gamma_h} d\Gamma_h = 0,$$

Convective Flux

$$\int_{\partial C_i} F(W_i^n).\mathbf{n}_i d\gamma = \sum_{v_j \in \vartheta(v_i)} F|_{I_{ij}}.\int_{\partial C_{ij}} \mathbf{n}_i d\gamma = \sum_{v_j \in \vartheta(v_i)} \Phi(W_i, W_j, \mathbf{n}_{ij}),$$

$$\Gamma_{ij} = \Gamma_{ij}(W_i, W_j, \mathbf{n}_{ij}) = F|_{I_{ij}}.\int_{\partial C_{ij}} \mathbf{n}_i d\gamma,$$

$$\Gamma_{ij}(W_i, W_j, \vec{\mathbf{n}}_{ij}) = \frac{F(W_i) + F(W_j)}{2}.\mathbf{n}_{ij} + d(W_i, W_j, \mathbf{n}_{ij}),$$

5. Extension to the Euler's equations (3)

Vertex, dual cell, 2-exact Central-ENO quadratic reconstruction

Given $\bar{u}_i$ on on each cell i of centroid G_i, find the $c_{i,\alpha}$, $|\alpha| \leq k$ such that

$$\overline{P_{i,i}} = \overline{W_i} \qquad \sum_{j \in N(i)} (\overline{P_{i,j}} - \overline{W_j})^2 = Min$$

with

$$P_i(x) = \bar{W}_i + \sum_{|\alpha| \leq k} c_{i,\alpha} [(X - G_i)^\alpha - \overline{(X - G_i)^\alpha}]$$

and where $\overline{P_{i,j}}$ stands for the mean of $P_i(x)$ on cell j.

Upwind Finite Volumes

$$\int_{\partial C_{ik}^{(1,2)}} F(W).\mathbf{n} d\gamma = \int_{\partial C_{ik}^{(1,2)}} F\Big(P_i(x,y,t)\Big).\mathbf{n} d\gamma.$$

$$\Phi(W_1, W_2, \mathbf{v}) = \frac{F(W_1) + F(W_2)}{2} \cdot \mathbf{v} - \frac{\dot{\gamma}}{2} \left| \frac{\partial F}{\partial \mathbf{v}} \left(\frac{W_1 + W_2}{2} \right) \cdot \mathbf{v} \right| (W_2 - W_1) \Big|.$$

Numerical comparisons : 1) advective

$$\begin{cases} \rho(x,y,0) = 20 + x + exp\left(-5\left(x - \frac{x_{min}+x_{max}}{2}\right)^2 - 5\left(y - \frac{y_{min}+y_{max}}{2}\right)^2\right) \\ u(x,y,t) = 1 \\ v(x,y,t) = 0 \\ p(x,y,t) = 2,51 \end{cases}$$

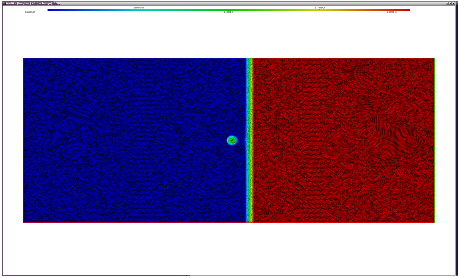

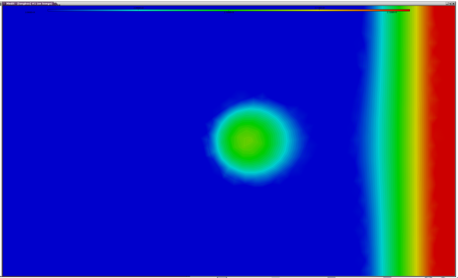

5. Extension to the Euler's equations (4)

Unstructured meshe (40 000 vertex), CFL 0.5

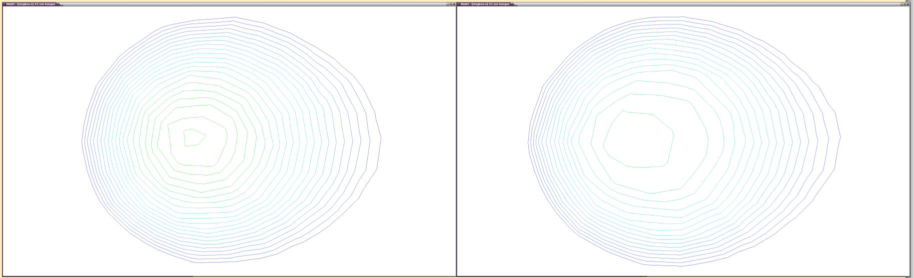

Quadratic scheme (left) and MUSCL V4 (right) for 500 iterations.

Numerical comparison : 2) acoustic

Acoustic source define by $f = (0,0,0,r)$ on a 50 000 nodes meshe :

$$r = -A.exp\big(-B.ln(2)[x^2+y^2]\big)C.cos(2\Pi fr),$$

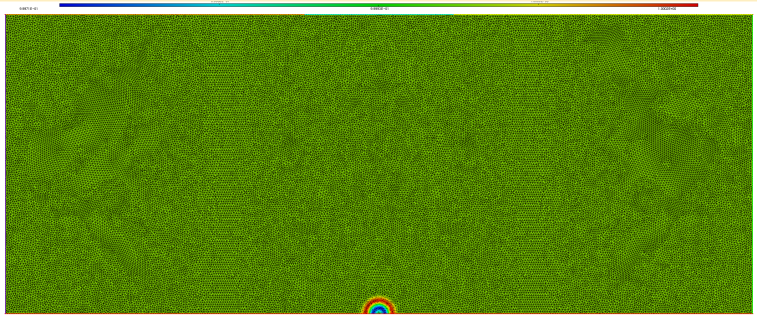

Muscl V4 (left), quadratic scheme (right), 500 iterations (top), 1000 iteratons (down)

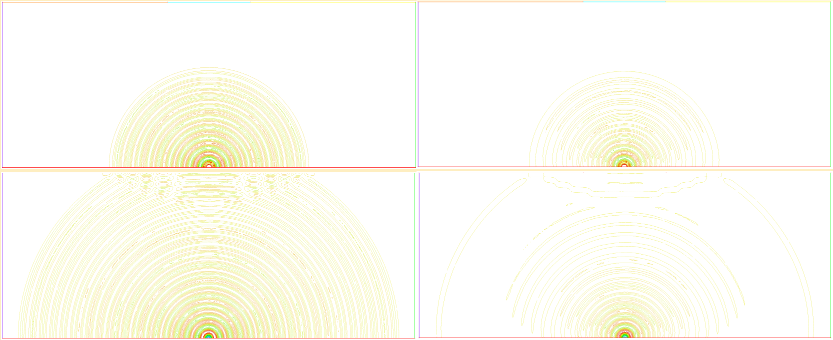

End. Concluding remarks

Synthesis

We are studying an advection scheme “for the poor”. It uses a quadratic reconstruction. 4 arithmetic means on Gauss integration points replace the 4 Riemann solvers. The rest of flux is made of two cheap HAEB-like terms.

Preliminary accuracy measures show a modest improvement in convergence order. The third-order baseline gives 2.91 to 2.92, the new scheme gives 3.12 to 4.1.

But the improvement is important in constants, for example, for unstructured meshes of 2,000 nodes, the error is 3,5 smaller, for 30,000 nodes, 6.5 times smaller.

What next

The new advection scheme will be experimented in combination with Hessian-based anisotropic mesh adaptation.

Thank you